Multivectorial paleointensity determination by the Thellier method

V. P. Shcherbakov[1] and G. V. Zhidkov[1]

Received 12 May 2006; revised 5 October 2006; accepted 12 October 2006; published 30 November 2006.

[1] Theoretical and experimental study of shape of the Arai-Nagata diagrams for the natural remanent magnetization (NRM) consisting of two low- and high-temperature partial thermal remanent magnetization vectors directed at angle θ to each other is considered. Assuming that the NRM is carried by single-domain and/or small pseudosingle-domain grains, that is, the Thellier laws of additivity and independence are valid, a theoretical consideration showed that the low-temperature portion of the diagram has a hyperbolic shape. A striking feature of the diagram is that at obtuse angle θ and strong enough low-temperature component it exhibits a minimum. The theoretical conclusions were examined experimentally; the results of the experiments are in a good agreement with the theoretical predictions. The shape of the low-temperature portion is predetermined by the angle θ, the relative intensity of low-temperature component, and the field h in which this component was imparted. These three parameters can be found from the results of Thellier experiments by the least squares method. It opens a way to determine the paleofield h and the angle θ which are characteristics of the low-temperature (presumably secondary) remanent magnetization. A few examples of such the determinations on samples from Proterozoic collections are reported.

Citation: Shcherbakov, V. P., and G. V. Zhidkov (2006), Multivectorial paleointensity determination by the Thellier method, *J. Geophys. Res.*, *111*, B12S32, doi:10.1029/2006JB004504.

1. Introduction

[2] The vector $\mathbf{M}_n$ of natural remanent magnetization (NRM) often consists of a sum of two (or more) vectors. For volcanic material it is commonly thought that the primary NRM is the thermal remanent magnetization (TRM) acquired in the ancient geomagnetic field $\mathbf{B}_{anc}$ during cooling from temperatures above the Curie temperatures T_c of the ferromagnetic minerals present in the rock. Secondary magnetizations are commonly induced by partly substituting the primary NRM by reheating in situ to elevated temperatures $T_m < T_c$ following by cooling to room temperature T_0 in an external field $\mathbf{B}_{sec}$. In such cases, these secondary magnetizations are partial TRMs (pTRM) acquired in the temperature interval (T_m, T_0). In the rest of the paper, for the sake of simplicity assume also that the NRM is carried by single-domain (SD) and/or small pseudosingle-domain (PSD) grains to ensure the validity of Thellier laws of additivity and independence. Under these laws, the total NRM vector $\mathbf{M}_n$ can be decomposed into the sum of low-temperature pTRM vector $\mathbf{M}_a$ with blocking temperatures $T_b \in \{T_m, T_0\}$ and high-temperature pTRM(T_c, T_m) vector $\mathbf{M}_b$, which is the remainder of the primary NRM.

[3] In general the fields $\mathbf{B}_{anc}$ and $\mathbf{B}_{sec}$ are different in both intensity and direction; the same is true for the vectors $\mathbf{M}_a$ and $\mathbf{M}_b$. Because of this "the slope of low-temperature portion of the Arai-Nagata plot will not give the correct paleofield intensity and may not even be linear" [*Yu and Dunlop*, 2002]. The purpose of the present work is to develop both theoretical and experimental study of Arai-Nagata diagrams for the case of NRM consisting of two complementary pTRM vectors.

2. Theory

[4] Let T_i (i = 1,2,...,n) be the sequence of ordered, ascending temperatures used in a Thellier experiment. In this paper we will consider the Thellier method of paleointensity determination as modified by *Coe* [1967]. Each T_i consists of a pair heating steps. During the first step a part ΔNRM of total the NRM is lost upon heating from T_0 to T_i in zero field. The second heating to T_i adds to the remaining remanence; a pTRM(T_0, T_i) = $I_{pt,i}$ acquired by cooling from T_i to T_0 in the laboratory field $\mathbf{B}_{lab}$. Remind that for multidomain and coarse PSD grains, the intensity of a pTRM(T_1, T_2) largely depends on the thermal prehistory of the sample. In main, two kinds of pTRMs are important. First, the upper temperature T_1 can be reached by cooling from T_c, this kind of pTRM is denoted as pTRM$_a$(T_1, T_2). Second, the sample can be initially thermally demagnetized by cooling in zero field from T_c to room temperature T_0, then heated to T_1 and cooled to T_2 in nonzero external field. Here the top temperature T_1 is reached by heating from T_0 to T_1 and this pTRM is called here as pTRM$_b$(T_1, T_2). The important difference between these two pTRMs is that pTRM$_a$(T_1, T_2) > pTRM$_b$(T_1, T_2) [*Shcherbakov et al.*, 1993; *Shcherbakova et al.*, 2000]. This difference must be taken in account when performing Thellier experiments as

[1]Geophysical Observatory "Borok" of Russian Academy of Sciences, Borok, Nekouzsky Region, Yaroslavskaya Oblast, Russia.

0148-0227/06/2006JB004504$09.00

the pTRMs induced during second heating to T_i are exactly of pTRM$_b$ type, while NRM is represented by a sum of pTRM$_a$. Fortunately, for SD and small PSD grains the difference between these pTRMs is negligible, besides, SD and small PSD grains obey the Thellier law of independence what was assumed already.

[5] Suppose now, that we deal with a two-component magnetization as described in the introduction. As follows from the law of independence of pTRMs, during this procedure only the low-temperature vector $\mathbf{M}_a$ will decay for until $T_i < T_m$. To analyze the effect of this demagnetization, consider the angle θ, which is the angle between the low-temperature $\mathbf{M}_a$ and high-temperature components $\mathbf{M}_b$ of the vector $\mathbf{M}_n$. Thus, according to the cosine theorem, the total vector at the condition $T_i \leq T_m$

$$M_{n,i}^2 = M_{a,i}^2 + M_b^2 + 2M_{a,i}M_b \cos\theta \quad (1)$$

Here $M_{n,i}$ and $M_{a,i}$ are absolute values of vectors $\mathbf{M}_n$ and $\mathbf{M}_a$, correspondingly, left after heating to T_i, $M_b = |\mathbf{M}_b|$. On the other hand, due to the linearity of value of pTRM in weak external magnetic fields and the independence of intensity of pTRM on the thermal prehistory for SD samples [*Shcherbakova et al.*, 2000]), one can also write

$$\frac{\Delta NRM_i}{M_{pt,i}} = \frac{B_{\mathrm{sec}}}{B_{lab}}, \quad T_i \leq T_m \quad (2)$$

where B_{sec} and B_{lab} are the absolute values of the corresponding vectors. Using equation (2) we obtain another relationship between $M_{a,i}$, M_a and $M_{pt,i}$:

$$M_{a,i} = M_a - M_{pt,i}\frac{B_{\mathrm{sec}}}{B_{lab}} \quad (3)$$

Introducing an expression for the normalized ancient field $h = B_{\mathrm{sec}}/B_{\mathrm{lab}}$ for the acquisition of the secondary magnetization, and combining equations (1) and (3) gives

$$B_{n,i}^2 = \left(B_a - B_{pt,i}h\right)^2 + B_b^2 + 2\left(B_a - B_{pt,i}h\right)B_b \cos\theta \quad (4)$$

Equation (4) shows that $M_{n,i}(M_{pt,i})$ dependence on the low-temperature portion of the Arai-Nagata diagram is nonlinear, having a hyperbolic shape. Its actual position on the Arai-Nagata diagram is determined by the three parameters: θ, M_a and h.

[6] Results of modeling Arai-Nagata diagrams for different angles θ and normalized fields h based on the equation (4) are shown in Figure 1. The values of magnetizations are normalized to total TRM acquired in the laboratory field. Following *Yu and Dunlop* [2002], it was assumed for the sake of simplicity that the high-temperature magnetization M_b (the rest of the "primary" NRM) was acquired in the same field as the laboratory one, i.e., $M_{\mathrm{anc}} = M_{\mathrm{lab}}$ ($B_{\mathrm{anc}} = |\mathbf{B}_{\mathrm{anc}}|$). This suggestion can be justified because if it is not true, it can still be achieved by scaling of the M_{pt} axis. For symmetry it was assumed $M_b = 0.5$. The other unknown in equation (4) is M_a. In Figure 1 its value is taken as $M_b h$ due to the assumptions $M_b = 0.5$ and $B_{\mathrm{anc}} = B_{\mathrm{lab}}$.

[7] Similar curves were computed by *Yu and Dunlop* [2002], but their calculations were done for angles $\theta = 60$, 90 and 180 degrees only. Occasionally, for the last (antiparallel) configuration only the case $M_a = M_b$ was considered when the low-temperature hyperbola degenerates in a straight line, so the Arai-Nagata diagram results in a combination of two straight lines. Hence the authors missed, perhaps, the most interesting case of obtuse angles θ when the diagrams ($M_{pt,i}$, $M_{n,i}$) have at certain condition a minimum in the low-temperature portion (Figure 1b). The position of the minimum can be found from the condition $\partial M_{n,i}/\partial M_{pt,i} = 0$, which is obtained by differentiation of equation (4) with respect to $M_{pt,i}$, giving

$$M_{pt,i}h = M_a + M_b \cos\theta \quad (5)$$

Taking into account that M_a, $M_{a,i}$ and $M_{pt,i}$ are positive, we obtain from (3) the inequality $M_{pt,i}h \leq M_a$. Consequently, as follows from equation (5), the minimum on the low-temperature portion of Arai-Nagata diagram can only occur for obtuse angles of θ, as stated above. The necessary condition for the appearance of the minimum is $M_a/M_b > -\cos\theta$. (As is evident, for the antiparallel case $\theta = 180°$ the minimum appears only at the condition $M_a > M_b$).

[8] Interestingly, if it is granted that the vector $\mathbf{M}_a$ vanishes at some $T_i = T_{cr}$ followed by a change in its direction to the opposite one as T_i increases, such a minimum can also occur at acute angles of θ. (This scenario is equivalent to the assumption that the angle θ abruptly jumps by π at T_{cr}; such an exotic possibility can occur if the low-temperature magnetization experiences a self-reversal.) Note that the transformations $\theta \rightarrow \pi - \theta$, $M_a \rightarrow M_a + 2M_b\cos\theta$ leave both expressions (4) and (5) unchanged. Formally it means that the corresponding Arai-Nagata diagrams are identical for the two sets of parameters satisfying these transformations. This phenomenon is illustrated in the inset in Figure 1b where the plot $M_{a,i}$ multiplied by the sign of $\cos\theta$ is shown as a function of $M_{pt,i}$. The dashed line in the inset shows the "normal" case $\theta = 135°$, $h = 3$, $M_b = 0.5$, $M_\Phi = M_b h = 1.5$ while the full line corresponds to the transformed set $\theta = 45°$, $h = 3$, $M_b = 0.5$, $M_a = 1.5 + 2 \cdot 0.5 \cdot \cos\theta = 1.5 - 1/\sqrt{2}$. As indicated in the inset, the full line shows typical self-reversal picture when the value of remanence changes sign during thermal demagnetization.

[9] According to (4), the shape of low-temperature portion of Arai-Nagata diagram is determined by the three parameters: the angle θ between the low- and high-temperature components of the vector $\mathbf{M}_n$, the intensity of low-temperature component M_a and the intensity of the normalized field h in which the magnetization $\mathbf{M}_a$ was acquired. Note that the value of M_b must be regarded as the known parameter. Indeed, its value is the NRM left after heating and subsequent cooling a sample to T_m in nonmagnetic space; thus it can be calculated directly from the Thellier experiment. On the other hand, the outcome of a Thellier experiment is a set of values ($M_{pt,i}$, $M_{n,i}$), $i = 1, N$, where N is the number of heatings of a sample up to the temperatures satisfying inequality $T_i \leq T_m$. As a rule, $N > 3$,

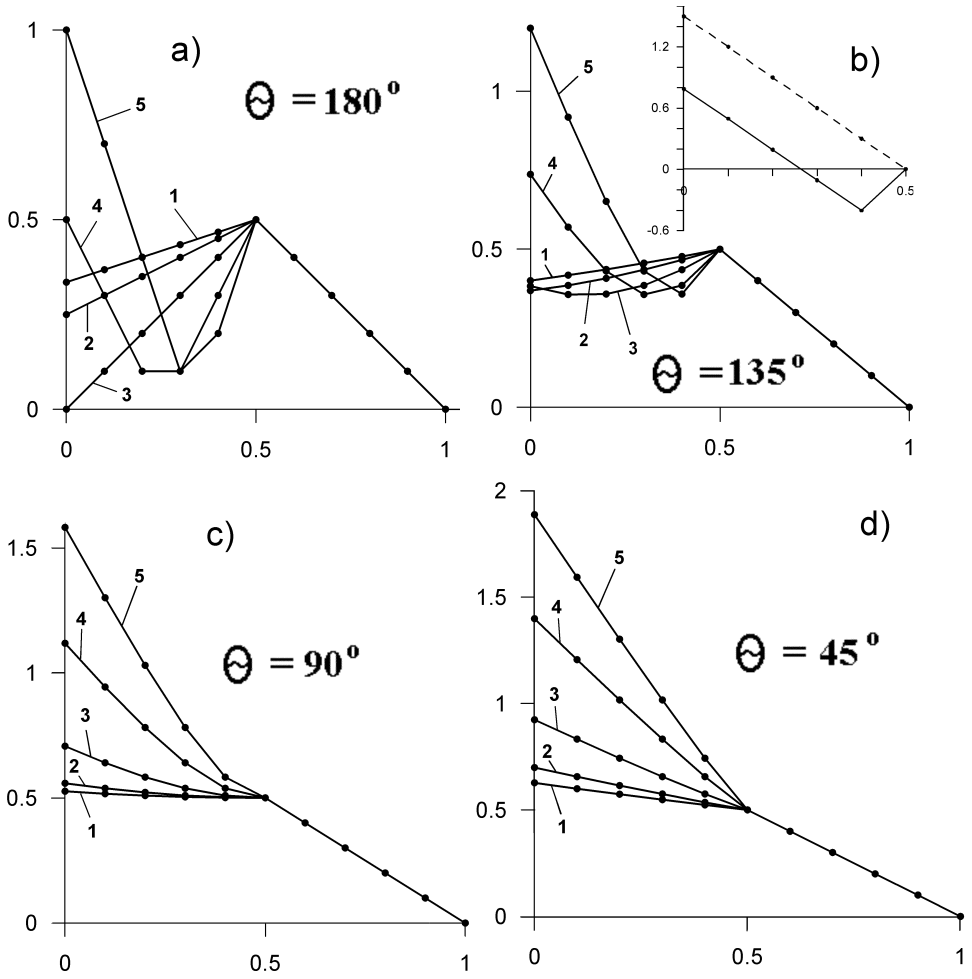

Figure 1. Arai-Nagata diagrams for $M_{n,i}$ against $M_{pt,i}$ calculated according to equation (4) for various angles θ and normalized field h. The values of θ are shown in each diagram, the numbers near the curves correspond to 1, h = 0.33; 2, h = 0.5; 3, = 1; 4, h = 2; 5, h = 3. The inset is $M_{a,i}$ versus $M_{pt,i}$ dependence for h = 3. The dashed line is for the "normal" case θ = 135°, while the solid line demonstrates the "self-reversal" case for θ = 45°.

making it possible to use the least squares method to find the parameters θ, M_a and h by minimization of the function

$$S(\theta, h, M_a) = \sum_{1}^{N} \cdot \left[M_{n,i} - \sqrt{\left(M_a - M_{pt,i}h\right)^2 + M_b^2 + 2\left(M_a - M_{pt,i}h\right)M_b \cos\theta} \right]^2 \quad (6)$$

Note that these calculations can be carried out before end of Thellier experiment, on the stage when the sample was heated to T_k only. In other words, determinations of the low-temperature paleofield can be done independently on its high-temperature counterpart.

3. Experiment

3.1. Sample Characterization

[10] A two-component induction coil thermomagnetometer was used for the experiments. The device allows to induce and to demagnetize full TRM or various pTRMs of different directions and to measure continuously the horizontal components of the remanent magnetic moment of a specimen rotating in the horizontal plane. The noise threshold of the magnetometer is 3×10^{-9} Am^2 for a cube specimen 1 cm^3 in size. The maximum available external field, whose direction is fixed in horizontal plane, is 0.2 mT, while the residual field, after the coil is switched off, is less than 100 nT.

[11] To examine experimentally the theoretical model proposed in the previous section, a thermally stabilized sample of Proterozoic basalt (PB) of 1450 Ma age from the Baltic shield, Karelia, Russia was taken. The Curie temperature of the sample determined on a Curie balance device in field 0.45 T is 575°C, indicating the presence of pure magnetite.

[12] As was mentioned above, the necessary requirement for the sample is the validity of the Thellier laws of additivity and independence of pTRMs. To identify the domain structure (DS), the common magnetic characteristics, such as saturation magnetization M_s, saturation rem-

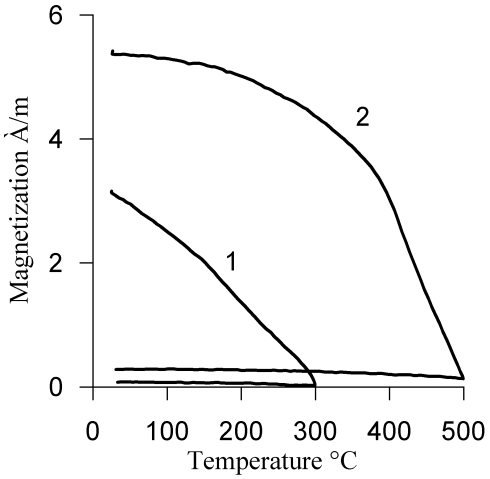

Figure 2. Thermal demagnetization curves of PB sample. Curves 1, pTRM (T_0, 300°C); 2, pTRM (400, 500)°C.

anence M_{rs}, coercive force B_c and remanent coercive force B_{cr} were measured. The values of ratios M_{rs}/M_s and B_{cr}/B_c for the PB sample are 0.11 and 1.65, correspondingly, indicating small PDS grains as the dominant magnetic carriers, that ensures validity of the Thellier laws as a first approximation.

[13] The DS was further examined by using the thermomagnetic criterion [*Shcherbakova et al.*, 2000; *Shcherbakov and Shcherbakova*, 2001] which estimates DS by thermal demagnetization of a pTRM, that is, this criterion is directly based on the Thellier law of independence. The result of the application of this criterion to the PB sample is shown in Figure 2. The pTRMa(T_0, 300)°C and $pTRM_b$(400, 500)°C were imparted on the two-component induction coil thermomagnetometer in B_{lab} = 50 μT, next each pTRM was partially thermal demagnetized by heating to the highest temperature of its creation followed by cooling to T_0 in zero field. The magnetic remanence was continuously measured during the heating-cooling cycles. The remanence remaining after this procedure is the so-called tail of pTRM. As is seen from the plots, the normalized (to total pTRM intensity) values of both tails are in the range (2.5–5)%, which is

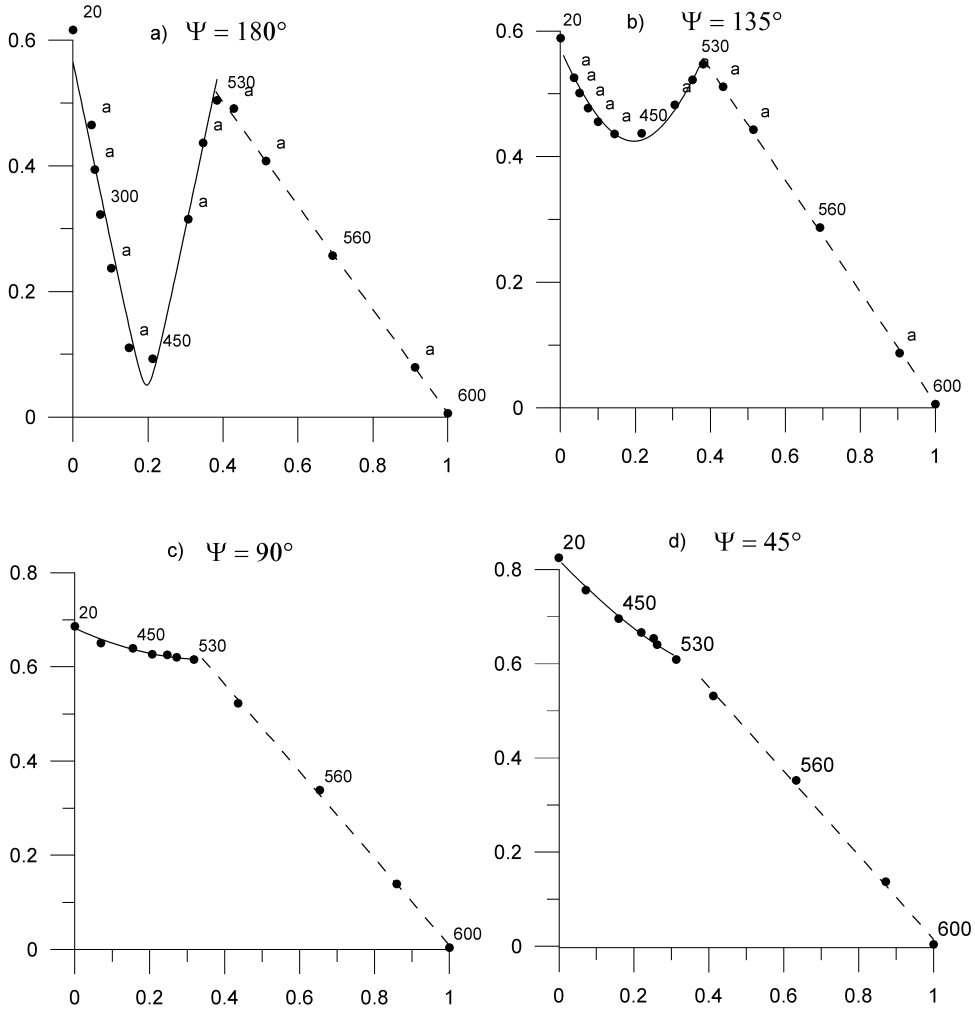

Figure 3. Arai-Nagata diagrams for the artificially induced two-component thermoremanent magnetization. The calculated θ and h are (a) θ = 179°; h = 1.43; (b) θ = 132°; h = 0.97; (c) θ = 90°; h = 0.83; (d) θ = 69°; h = 1.13.

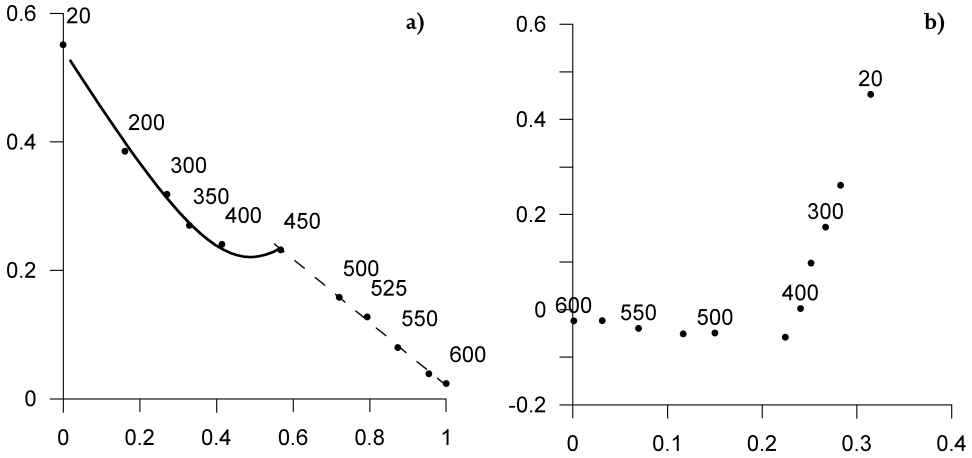

Figure 4. Sample F01. The laboratory field B_{lab} used in this experiment was 20 μT. (a) Arai-Nagata diagram. The solid line gives the hyperbolic fit for the high-temperature component, and the dashed line presents the linear fit for the high-temperature portion of the diagram. (b) Orthogonal projection.

characteristic for small PSD grains [*Shcherbakov and Shcherbakova*, 2001].

3.2. Paleointensity Experiments

[14] In order to simulate the paleointensity experiments with a two-component remanent magnetization, first the PB sample was given a total TRM in laboratory field H_{lab}. This magnetization obviously plays the role of NRM. Then the sample was rotated in the horizontal plane for a given angle ψ, reheated to 530°C and cooled down to T_0 in an external field, which we for the convenience denote as B_{anc}. Both these fields was different for different experiments, for the acute rotation angles ψ = 45 and 90 degrees it was assigned as $B_{lab} = B_{anc} = 50$ μT (the reduced field is $h = 1$). For $\psi = 135°$ and $\psi = 180°$ it was used $B_{lab} = B_{anc} = 100$ μT ($h = 1$) and $B_{lab} = 100$ μT, $B_{anc} = 150$ μT ($h = 1.5$), correspondingly. The magnetization obtained was subjected to Thellier experiments. Representative results are shown in Figure 3. All values of the magnetization in each diagram are normalized to the total TRM. The squares correspond to experimental points, the full lines show the fitting curves calculated according to equation (4). The full lines give the hyperbolic fit for the low-temperature components, and the dashed lines present the linear fit for the high-temperature portions of the diagrams. The figures near the points indicate the temperature step of the Thellier procedure, the value of ψ on each diagram depicts the designated angle between the low- and high-temperatures magnetization components used in the particular experiment. The fitting parameters θ, M_a and h involving in this formula were found by minimization of the function (6). The results show a good agreement between the calculated and designated angles and fields, especially at obtuse and right angles. Indeed, the values of calculated rotation angle θ is very close to the designated one ψ, the agreement between the calculated and designated reduced field h is also rather good. However, for the acute ψ the errors in fitted parameters increase as exemplified in Figure 3d. The reason for this is obvious – the difference in shape between the low- and high-temperatures portions of the diagrams there is not strongly expressed as it takes place for the obtuse angles.

3.3. Application of the Method to Natural Samples

[15] The results discussed below were obtained using a full vector three-component thermal magnetometer constructed in the Geophysical Observatory "Borok", Russia. The device performs completely automated Thellier procedures, that allows to carry out experiments on different samples under exactly the same algorithm and makes paleointensity determinations free of subjective errors. The sensitivity of the magnetometer is 10^{-8} A m^2 for a cube specimen 1 cm^3 in size. The maximum available external (vertical) field is 0.2 mT.

[16] The purpose of experiments was to apply the method to samples carrying fresh NRM and, to check the ability of the method to obtain results of paleomagnetic significance. The first task was to estimate the paleointensity at the time of acquisition of the secondary magnetization.

[17] With this aim, the results of Thellier experiments of more than two hundred samples from collections of Proterozoic samples collected in Karelia (1450 Ma age) and southeast Siberia (dated at 1850 Ma) were thoroughly revised. These collections were chosen because a palaeomagnetic study of these collections (the results of this study will be reported elsewhere), clearly showed that a number of samples carry multicomponent NRM [*Pavlov*, 2006; V. V. Shcherbakova et al., Paleomagnetism and paleointensity of the early Riphean dyke complexes of lake Ladoga region, submitted to *Izvestiya, Physics of the Solid Earth*, 2006, hereinafter referred to as Shcherbakova et al., submitted manuscript, 2006]. Unfortunately on revision of the data only a few samples demonstrated Arai-Nagata plots shaped closely to those of Figures 1 and 3. In addition, it must be noted that the temperature T_m which is characteristic for Arai-Nagata diagrams was not always identical to the turning temperature T_z seen on orthogonal plots. This makes it impossible to use such the diagrams for modeling.

[18] In total, two successful results were obtained from the southeast Siberian collection and four more from the Karelian collection; two cases are shown in Figures 4 and 5. Curie temperatures of the Siberian samples are in the range 580–600°C, indicating that the magnetite in these samples is partly oxidized to cation-deficient mineral. The Karelian

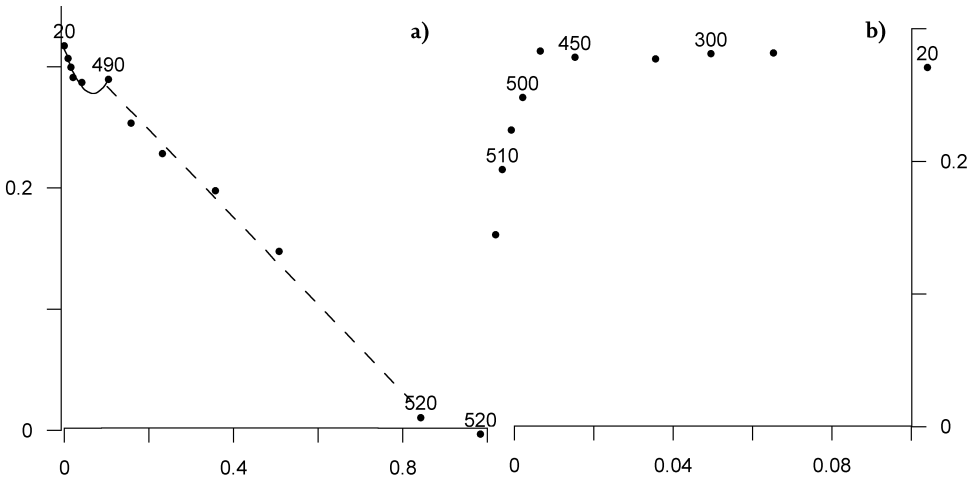

Figure 5. Sample St3. The laboratory field B_{lab} used in this experiment was 50 μT. The diagrams and notation are the same as for the Figure 4.

samples have T_c in the range 540–560°C, which is typical for low titanium magnetite. The ratios M_{rs}/M_s and B_{cr}/B_c for all these samples lie in the ranges 0.1–0.2 and 1.7–2.5, correspondingly, indicating presence of PSD states. For the sake of simplicity the orthogonal plots are shown in one plane only, arranged in such the way that the perpendicular component is small. For the same reason of simplicity, we omitted the pTRM check points, which for these samples are close to the corresponding initial points on the Arai-Nagata diagrams to within 10% (the test for the pTRM check is positive). Note also that the values of magnetization in the diagrams in Figures 4 and 5 are normalized to the NRM value of the corresponding samples.

[19] Figure 4 presents the Arai-Nagata diagram and orthogonal plot for the sample F01 collected in southeast Siberia. Both critical temperatures T_m and T_z equal 450°C, the Proterozoic paleointensity H_{anc} determined from the high-temperature component is 24 μT. *Pavlov* [2006] argued that the secondary component was induced during the Mesozoic epoch (more exact dating is not available). The best fit parameters B_{sec} and θ were calculated according to the algorithm developed above. The angle θ was found using this method to be 106° which is not far from the angle $\psi = 93°$ determined form the orthogonal plot. The paleointensity B_{sec} that in our model represents the Mesozoic field, equals 51 μT.

[20] The Karelian samples were taken from a dike, which is a part of a dike field near town Sortavala. Both the dike and surrounding rocks show distinctive two-component NRM. The paleopole calculated from the low-temperature component of NRM is close to that of Devonian for the East Russian platform (Shcherbakova et al., submitted manuscript, 2006). Figure 5 demonstrates the Arai-Nagata and orthogonal projection plots for the sample St3 from the dike. As the Siberian sample F01, St3 also gives low Proterozoic field B_{anc} about 8 μT determined from the high-temperature portion (490, 520)°C of the Arai-Nagata plot. The low-temperature component of NRM was induced in temperatures less than 490°C. The best fitting paleointensity B_{sec} for this component is 40 μT, the angle $\theta = 106°$. In comparison the angle between the high- and low-temperature components calculated from the orthogonal plot (Figure 5b) is $\psi = 104°$ which is in an excellent agreement for the value of θ.

4. Discussion and Conclusions

[21] Following the approach of *Yu and Dunlop* [2002, 2006], the Arai-Nagata plot for NRMs consisting of a sum of two vectors are studied both theoretically and experimentally. Assuming that NRM consists of two complementary pTRM vectors and the sample exhibits ideal SD behavior, it is shown that the low-temperature segment of the Arai-Nagata plot has a hyperbolic shape. On the basis of this property, a best fit procedure to determine the intensity of the field inducing the low-temperature component of the NRM is suggested.

[22] In the approach presented here, the angle θ between the two magnetization vectors is treated as an unknown, though it is commonly known from the orthogonal projection plot if the sample was subjected to paleodirection determinations which is usually the case. Then, a modification of the method can be offered when the least squares method is applied to the equation (6) to find only two parameters: B_a and h. Moreover, as far as value of B_a can be retrieved from the stepwise demagnetization data, one can determine the magnitude and orientation of the overprint directly from equation (1) taken at room temperature. Then, using these quantities and the intensity of pTRM(T_0, T_m) imparted in laboratory field B_{lab}, one can easily calculate the ancient overprinting field. This simplified version seems to be more practical, but the procedure based on the least squares method has at least two advantages. First, it delivers much more reliable paleointensity determinations as it uses not only the magnetization data obtained at room temperature, but the whole set of the data taken at elevated temperatures. Second, an encouraging feature of this method is that its performance includes the determination of the angle θ between the low- and high-temperature components of the NRM vector. This provides an additional independent test of reliability of the method by comparison of θ and corresponding angle ψ between the components obtained independently from the orthogonal projection plot. Finally,

the best fit procedure suggested here is authentic to the Thelleir method for the case of single-component magnetization while the simplified version is actually similar to the paleointensity determinations based on the calculation of the ratio NRM/TRM. However, such the data are usually disregarded now as being basically unreliable.

[23] A few paleointensity determinations on natural Paleozoic samples, for which the agreement between θ and ψ was satisfactory, were obtained by the new proposed method. It should be noted, that for all these samples the orthogonal projection plots shows a sharp turn from one direction to another. This means that the blocking temperatures of the two components do not overlap; hence it is unlikely that the low-temperature component is of chemical origin but its appearance is more likely due to thermal overprinting of the preexisting NRM. With regard to the paleomagnetic significance of paleointensity determinations for Mesozoic and Late Paleozoic reported here, it seems clear that at this stage of research it is too preliminary to discuss whether or not these determinations reflect the true intensity of the ancient field. For all six successful cases the paleointensity B_{sec} attributed to the secondary low-temperature component occurred to be relatively high, between about 40 and 50 μT.

[24] **Acknowledgments.** This research was sponsored by the Russian Fund of Basic Researches, grant 06-05-64538. The authors are grateful to M. Jackson and Y. Yu for stimulating discussions and suggestions.

References

Coe, R. S. (1967), The determination of paleointensities of the Earth magnetic field with special emphasize on mechanisms which could cause nonideal behavior in Thelliers method, *J. Geomagn. Geoelectr.*, *19*, 157–179.

Pavlov, V. E. (2006), Birthplace of the Siberian platform, in *Regions of Active Tectonogenesis in Modern and Ancient Earth's History*, pp. 88–91, Moscow State Univ., Moscow.

Shcherbakov, V. P., and V. V. Shcherbakova (2001), On suitability of the Thellier method of paleointensity determinations to pseudosingledomain and multidomain grains, *Geophys. J. Int.*, *146*, 20–30.

Shcherbakov, V. P., E. McClelland, and V. V. Shcherbakova (1993), A model of multidomain thermoremanent magnetization incorporating temperature-variable domain structure, *J. Geophys. Res.*, *98*, 6201–6216.

Shcherbakova, V. V., V. P. Shcherbakov, and F. Heider (2000), Properties of partial thermoremanent magnetization in PSD and MD magnetite grains, *J. Geophys. Res.*, *105*, 767–782.

Yu, J., and D. J. Dunlop (2002), Multivectorial paleointensity determinations from the Cordova gabbro, southern Ontario, *Earth Planet. Sci. Lett*, *203*, 983–998.

Yu, Y., and D. J. Dunlop (2006), Testing the independence of partial thermoremanent magnetizations of single-domain and multidomain grains: Implications for paleointensity determination, *J. Geophys. Res.*, *111*, B12S31, doi:10.1029/2006JB004434.

V. P. Shcherbakov and G. V. Zhidkov, Geophysical Observatory "Borok" of Russian Academy of Sciences, Borok, Nekouzsky region, Yaroslavskaya oblast, 152742, Russia. (shcherbakovv@list.ru)